



ELSEVIER

Journal of Alloys and Compounds 336 (2002) 265–269

Journal of
ALLOYS
AND COMPOUNDS

www.elsevier.com/locate/jallcom

Nanocrystalline titanium-type metal hydride electrodes prepared by mechanical alloying

M. Jurczyk^{a,*}, E. Jankowska^b, M. Nowak^a, J. Jakubowicz^a^a*Institute of Materials Science and Engineering, Poznan University of Technology, M. Skłodowska-Curie 5 Sq., 60-965 Poznan, Poland*^b*Central Laboratory of Batteries and Cells, Forteczna 12/14 St., 61-362 Poznan, Poland*

Received 10 September 2001; accepted 19 September 2001

Abstract

Mechanical alloying (MA) was employed to produce nanocrystalline $\text{TiFe}_{1-x}\text{Ni}_x$ alloys ($x=0, 0.25, 0.5, 0.75$ and 1.0). XRD analysis showed that, after 25 h of milling, the starting mixture of the elements had decomposed into an amorphous phase. Following annealing in high purity argon at 750°C for 0.5 h, XRD confirmed the formation of the CsCl-type structures with crystallite sizes of about 50 nm. These materials were used as negative electrodes for a Ni–MH_x battery. With increasing nickel content in $\text{TiFe}_{1-x}\text{Ni}_x$, the material shows an increase in discharge capacity which passes through a maximum for $x=0.75$. In the nanocrystalline $\text{TiFe}_{0.25}\text{Ni}_{0.75}$ powder, discharge capacities of up to 155 mA h g^{-1} (at 40 mA g^{-1} discharge current) were measured. The titanium-based hydrogen storage alloys are attractive for secondary batteries, because of inexpensive raw materials. © 2002 Elsevier Science B.V. All rights reserved.

Keywords: Transition metal compounds; Hydrogen absorbing materials; Electrode materials; Mechanical alloying

1. Introduction

Mechanical alloying (MA) has proved to be a novel and promising method for alloy formation, especially in the preparation of non-equilibrium materials of various systems [1–7]. This technique has already succeeded in synthesising a wide range of alloy hydrides for energy storage or other energy-related applications [4–9]. The advanced nanocrystalline intermetallics represent a new generation of metal hydride materials with the following characteristics: high storage capacity, stable temperature–pressure cycling capacity during the life-time of the system, good corrosion stability and low cost.

These materials exhibit quite different properties from both crystalline and amorphous materials, due to structure in which extremely fine grains are separated by what some investigators have characterized as ‘glass-like’ disordered grain boundaries [2,3]. Therefore, the hydrogenation behaviour of the amorphous structure is different from that of the crystalline material. MA has recently been used to make amorphous and nanocrystalline Mg_2Ni -, ZrV_2 - and LaNi_5 -type alloys [4–7]. These materials show substantial-

ly enhanced absorption and desorption kinetics, even at relatively low temperatures [5].

Among the different types of hydrogen forming compounds, Ti-based alloys are promising materials for hydrogen energy applications [5,10,11]. For example, the TiFe alloy, which crystallizes in the cubic CsCl-type structure, is lighter and cheaper than the LaNi_5 -type alloys and can absorb up to 2 H/f.u. at room temperature. It is a nontoxic material. Nevertheless, the application of TiFe material in batteries has been limited due to poor absorption/desorption kinetics in addition to a complicated activation procedure. To improve the activation of this alloy several approaches have been adopted. For example, the replacement of Fe by some amount of transition metals to form a secondary phase may improve the activation property of TiFe [12,13]. After activation, the TiFe reacts directly and reversibly with hydrogen to form two ternary hydrides TiFeH (orthorhombic) and TiFeH_2 (monoclinic), each of which is a distorted form of the b.c.c. structure of the unhydrided alloy [11]. In addition, excess Ti in TiFe, i.e. Ti_{1+x}Fe enables the alloy to be hydrided without the activation treatment. On the other hand, ball milling of TiFe is effective for the improvement of the initial hydrogen absorption rate, due to the reduction in the particle size and to the creation of new clean surfaces [14,15].

*Corresponding author. Tel.: +48-61-835-1647; fax: +48-61-665-3576.

E-mail address: jurczyk@sol.put.poznan.pl (M. Jurczyk).

In this work, the structural and electrochemical properties of nanocrystalline $\text{TiFe}_{1-x}\text{Ni}_x$ ($x=0, 0.25, 0.5, 0.75$ and 1.0) alloys were investigated. The materials produced by MA and subsequent annealing with 10 wt% addition of Ni powder, were subjected to electrochemical measurements as working electrodes. Surprisingly, the influence of nickel content on electrochemical behaviour of the nanocrystalline $\text{TiFe}_{1-x}\text{Ni}_x$ alloys has not been investigated in detail.

2. Experimental

MA was carried out under an argon atmosphere using a SPEX 8000 D Mixer Mill. The purity of the starting metallic elements Ti, Fe and Ni was 99, 99.5 and 99.9 wt%, respectively. The composition of the starting powder mixture corresponded to the stoichiometry of the ‘ideal’ reactions. The elemental powders (Ti: $\leq 45 \mu\text{m}$, Fe: $\leq 10 \mu\text{m}$; Ni: $3\text{--}7 \mu\text{m}$ — all from Johnson Matthey Company) were mixed in a glove box (Labmaster 130) and poured into a vial. The mill was run up to 30 h for each powder preparation. The as-milled powders were heat-treated at 750°C for 0.5 h under high purity argon to form the regular CsCl-type phase. The MA process of the $\text{TiFe}_{1-x}\text{Ni}_x$ mixtures has been studied by X-ray diffraction (XRD) and scanning electron microscopy (SEM). The crystallization behaviour of the mechanically alloyed materials was examined by differential scanning calorimetry (DSC 404, Netzsch). Typical crystallite sizes were estimated from the half-width of lines using the Scherrer equation. The change in the structure of powdered samples was examined using Atomic Force Microscopy (Nanoscope IIIa — Digital Instruments, USA). The AFM contact mode with conical Si tip has been applied. A square scan size in the range of $2 \times 2 \mu\text{m} \text{--} 100 \times 100 \text{ nm}$ with a resolution of 512×512 pixels has been used. The powder was fixed to the metal plate put on the piezoelectric scanner. Measurements were done in air.

The mechanically alloyed and annealed (nanocrystalline) materials with 10 wt% addition of Ni powder, were subjected to electrochemical measurements as working electrodes after pressing (under 80 kN cm^{-2}) to a 0.5-g pellet form between nickel nets acting as current collector. The diameter of each electrode was 10.4 mm and the thickness approximately 1.4 mm. Soaking of the electrodes in 6 M KOH solution for 24 h at room temperature with additional etching at 100°C for 10 min in the same solution was sufficient for the initial activation. The electrochemical properties of electrodes were measured in a three-compartment glass cell, using a much larger $\text{NiOOH}/\text{Ni}(\text{OH})_2$ counter electrode and a $\text{Hg}/\text{HgO}/6 \text{ M KOH}$ reference electrode. All electrochemical measurements were carried out in deaerated 6 M KOH solution prepared from Analar grade KOH and $18 \text{ M}\Omega \text{ cm}^{-1}$ water, at 20°C . Potentiodynamic and galvanostatic techniques with either

short or long-term pulses using a conventional apparatus were applied to study the charge–discharge kinetics of the electrodes. A detailed description of the electrochemical measurements was given in Ref. [9].

3. Results and discussion

The behaviour of MA process has been studied by X-ray diffraction, microstructural investigations, AFM as well as by electrochemical measurements. Fig. 1 shows a series of XRD spectra of mechanically alloyed Ti–Fe powder mixture (53.85 wt% Ti+46.15 wt% Fe) subjected to milling for increasing time. The originally sharp diffraction lines of Ti and Fe gradually become broader (Fig. 1a) and their intensity decreases with milling time. The powder mixture milled for more than 25 h has transformed completely to the amorphous phase, without formation of another phase (Fig. 1c). During the MA process the crystallite size of the Ti decreases with MA time and reaches a steady value of 35 nm after 15 h of milling. This size of the crystallites seems to be favourable for the formation of an amorphous phase, which develops at the Ti–Fe interfaces. Formation of the nanocrystalline alloy TiFe was achieved by annealing the amorphous material in a high purity argon atmosphere at 750°C for 0.5 h (Fig. 1d). All diffraction peaks were assigned to those of the CsCl-type structure with cell parameter $a=2.973 \text{ \AA}$. When nickel is added to $\text{TiFe}_{1-x}\text{Ni}_x$ the lattice constant a increases (Table 1).

Using TiFe and TiNi, the amorphization process was also studied by DSC. After MA, the DSC curves stabilized exhibiting one exothermic effect at 692°C (Fig. 2) and

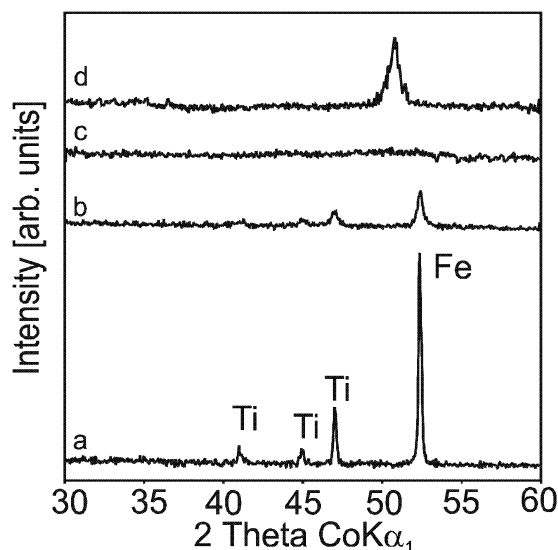


Fig. 1. XRD spectra of a mixture of Ti and Fe powders mechanically alloyed at different times in an argon atmosphere: (a) initial state (elemental powder mixture); (b) after MA for 5 h; (c) after MA for 25 h and (d) heat-treated at 750°C for 0.5 h.

Table 1
Structural parameters and discharge capacities for nanocrystalline $\text{TiFe}_{1-x}\text{Ni}_x$ materials

Composition	a (Å)	V (Å ³)	Discharge capacity on third cycle (mA h g ⁻¹)
TiFe	2.973	26.28	0.7
$\text{TiFe}_{0.75}\text{Ni}_{0.25}$	2.991	26.76	55
$\text{TiFe}_{0.5}\text{Ni}_{0.5}$	3.001	27.03	125
$\text{TiFe}_{0.25}\text{Ni}_{0.75}$	3.010	27.27	155
TiNi	3.018	27.49	67

Current density of charging and discharging was 40 mA g⁻¹.

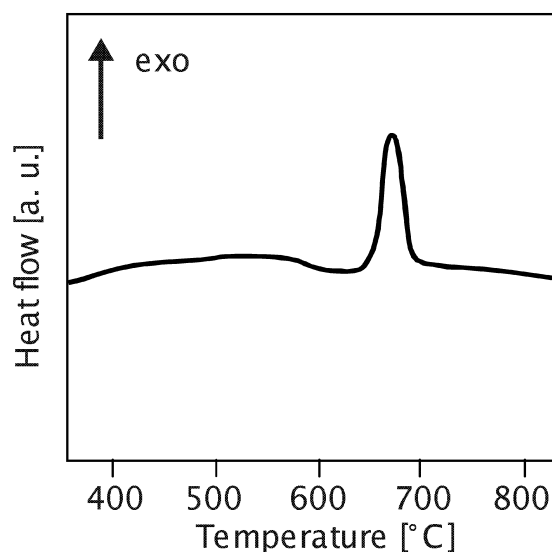


Fig. 2. DSC curve for an amorphous Ti–Fe mixture after 25 h MA (heating rate in argon: 20°C min⁻¹).

460°C for TiFe and TiNi, respectively. Taking into account XRD results, one can assume that these effects are attributed to the crystallization of the amorphous phases formed during the MA process. The results obtained are in good agreement with earlier work [2].

The SEM technique was used to follow the changes in size and shape of the mechanically alloyed powder mixtures as a function of milling time. As soon as the MA process is started, the powder particles which are trapped between colliding balls, are subjected to compressive impact forces. The powder particles are deformed, fractured and cold-welded [1,3]. The microstructure that forms during MA consists of layers of the starting material. The lamellar structure is increasingly refined during further MA. The thickness of the material decreases with the increase in MA time leading to true alloy formation. The sample shows cleavage fracture morphology and inhomogeneous size distribution. Many small powder particles have a tendency to agglomerate. Fig. 3 shows a SEM micrograph of typical Ti and Fe particles after 25 h of milling (Fig. 3). The average crystallite size of the nanocrystalline TiFe powders, according to AFM studies, was of the order of 50 nm (Fig. 4).

Table 1 reports the discharge capacities of the materials studied. The discharge capacity of the electrodes prepared by application of MA TiFe alloy powder is very low (Fig. 5). Materials obtained when Ni was substituted for Fe in $\text{TiFe}_{1-x}\text{Ni}_x$ lead to a great improvement in activation behaviour of the electrodes. It was found that the increasing nickel content in $\text{TiFe}_{1-x}\text{Ni}_x$ alloys leads initially to an increase in discharge capacity, giving a maximum at $x=0.75$. In the annealed nanocrystalline $\text{TiFe}_{0.25}\text{Ni}_{0.75}$ powder, discharge capacities of up to 155 mA h g⁻¹ (at 40 mA

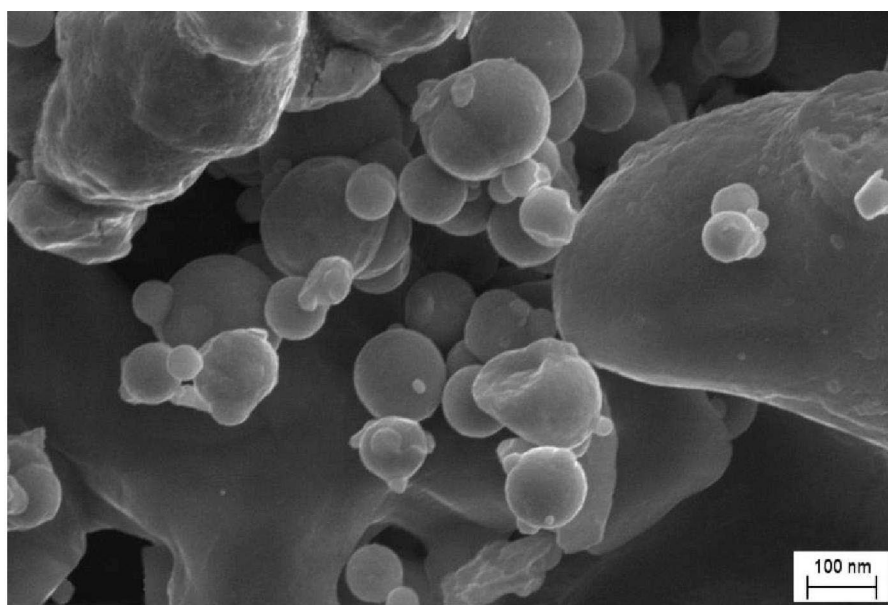


Fig. 3. SEM of a mixture of Ti and Fe powders mechanically alloyed for 25 h under argon atmosphere (original magnification: $\times 1000$).

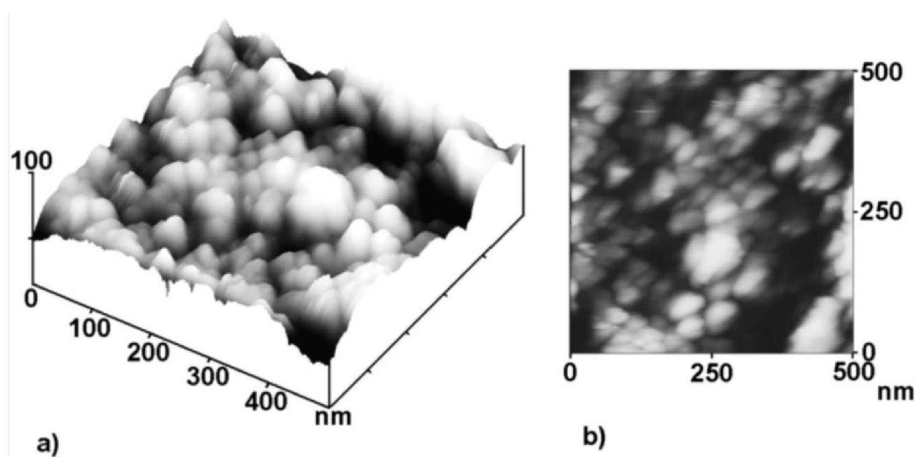


Fig. 4. AFM photographs of a mixture of Ti and Fe powders mechanically alloyed for 25 h under argon atmosphere.

g^{-1} discharge current) were measured, which compares with 161 mA h g^{-1} reported earlier for mechanically alloyed $\text{TiFe}_{0.4}\text{Ni}_{0.6}$ powder [15]. The electrodes obtained by MA and annealing of the elemental powders displayed maximum capacities at around the third cycle but, especially for $x=0.5$ and 0.75 in the $\text{TiFe}_{1-x}\text{Ni}_x$ alloy, degraded slightly with cycling. This may be due to the easy formation of an oxide layer (TiO_2) during the cycling.

On the other hand, it is important to note that the mechanically alloyed TiFe alloys showed higher discharge capacities than the arc melted ones [16]. The size reduction of the powder particles and the creation of new surfaces are effective for the improvement of the hydrogen absorption rate.

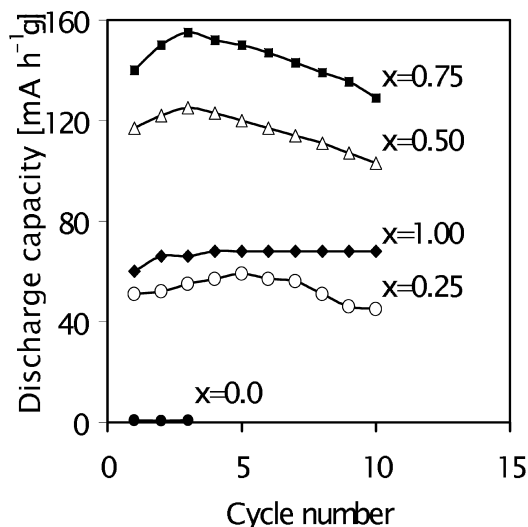


Fig. 5. Discharge capacities as a function of cycle number of electrode prepared with nanocrystalline $\text{TiFe}_{1-x}\text{Ni}_x$ (solution, 6 M KOH; temperature, 20°C). The charge conditions were 40 mA g^{-1} . The cut-off potential versus $\text{Hg}/\text{HgO}/6 \text{ M KOH}$ was -0.7 V .

4. Conclusion

In conclusion, nanocrystalline $\text{TiFe}_{1-x}\text{Ni}_x$ alloys synthesized by MA and annealing were used as negative electrode materials for a Ni–MH_x battery. The discharge capacity of electrodes prepared by application of MA and annealing of TiFe alloy powder displayed very low capacity (0.7 mA h g^{-1}). It was found that the increasing nickel content in $\text{TiFe}_{1-x}\text{Ni}_x$ alloys leads initially to an increase in discharge capacity, giving a maximum at $x=0.75$. In the nanocrystalline $\text{TiFe}_{0.25}\text{Ni}_{0.75}$ powder, discharge capacities of up to 155 mA h g^{-1} (at 40 mA g^{-1} discharge current) were measured. MA is a suitable procedure to obtain Ti-based alloy powders.

Acknowledgements

The financial support of the Polish National Committee for Scientific Research (KBN) under the contract No KBN 8T10A 001 20 is gratefully acknowledged. The Labmaster 130 (M. Braun) glove box was purchased by the Foundation for Polish Science under the program TECHNO-2000.

References

- [1] J.S. Benjamin, *Sci. Am.* 40 (1976) 234.
- [2] J. Eckert, L. Schultz, K. Urban, *J. Non-Cryst. Solids* 127 (1991) 90.
- [3] H. Gleiter, *Prog. Mater. Sci.* 33 (1989) 223.
- [4] A. Anani, A. Visintin, K. Petrov, S. Srinivasan, J.J. Reilly, J.R. Johnson, R.B. Schwarz, P.B. Desch, *J. Power Sources* 47 (1994) 261.
- [5] L. Zaluski, A. Zaluska, J.O. Ström-Olsen, *J. Alloys Comp.* 253–254 (1997) 70.
- [6] M. Jurczyk, W. Rajewski, G. Wojcik, W. Majchrzycki, *J. Alloys Comp.* 285 (1999) 250.

- [7] M. Jurczyk, W. Rajewski, W. Majchrzycki, G. Wojcik, J. Alloys Comp. 290 (1998) 264.
- [8] M. Jurczyk, W. Majchrzycki, J. Alloys Comp. 311 (2000) 311.
- [9] W. Majchrzycki, M. Jurczyk, J. Power Sources 93 (2001) 77.
- [10] K.H.J. Buschow, P.C.P. Bouten, A.R. Miedema, Rep. Prog. Phys. 45 (1982) 937.
- [11] D.H. Bradhurst, Metals Forum 6 (1983) 139.
- [12] B. Luan, N. Cui, H.K. Liu, H.J. Zhao, S.X. Dou, J. Power Sources 55 (1985) 197.
- [13] S.M. Lee, T.P. Perng, J. Alloys Comp. 291 (1999) 254.
- [14] H. Aoyagi, K. Aoki, T. Masumoto, J. Alloys Comp. 231 (1995) 804.
- [15] C.B. Jung, J.H. Kim, K.S. Lee, Nanostruct. Mater. 8 (1997) 1093.
- [16] C.B. Jung, K.S. Lee, J. Alloys Comp. 253–254 (1997) 605.